SciRad SCIENTIAE RADICES

Unveiling substituent effects in [3+2] cycloaddition reactions of benzonitrile N-oxide and benzylideneanilines from the molecular electron density theory perspective

Asmita Mondal[(1)], Haydar A. Mohammad-Salim[(2)], Nivedita Acharjee[(1)] ✉

[(1)] Department of Chemistry, Durgapur Government College, Durgapur-713214, West Bengal, India.
[(2)] Department of Chemistry, University of Zakho, Duhok 42001, Iraq.

✉ Correspondence to: nivchem@gmail.com

Abstract: The *zw- type* [3+2] cycloaddition (32CA) reactions of benzonitrile N-oxide with a series of substituted benzylideneanilines have been studied within the Molecular Electron Density Theory (MEDT) at the B3LYP/6-31G(d) computational level. The presence of dimethylamino and methoxy substituents in the aromatic rings of benzylideneaniline makes the reaction more facile relative to the unsubstituted one, while the electron withdrawing nitro substituents relatively induce minimal changes in the energy profile complying with the experimentally observed reaction rates. The presence of non-bonding electron density at the nitrogen atom and the formation of *pseudoradical* centre at the carbon atom of benzonitrile N-oxide characterise the difference in electronic structure of the TSs relative to the reagents, while the topological analysis of the electron localization function (ELF) and the atoms-in-molecules (AIM) reveal no covalent bond formation at the early TSs. The present MEDT study analyses the experimentally observed substituent effects and complete regioselectivity in the studied 32CA reactions.

Keywords: Benzonitrile N-oxide, Benzylideneanilines, Electron Localization Function, [3+2] cycloaddition reactions, MEDT

Introduction

The [3+2] cycloaddition [1] (32CA) reactions represent a well-documented field of research owing to the diverse applications of the generated adducts in academia and industry[2]. These reactions involve addition of a three atom component (TAC) to a multiple bond system for the construction of five-membered heterocycles [1-3]. Although the 32CA reactions of TACs with alkenes and alkynes have received widespread attention [1-3], the heteronuclear double bonds also serve as excellent reaction counterparts for the obtainment of synthetically useful heterocycles [4,5]. The 32CA reactions of benzonitrile N-oxide (BNO) **1** with the azomethine double bond of benzylideneanilines **2-5** provide easy synthetic route to 1,2,4-oxadiazolines [6] (Scheme 1). Alcaide et al. [6] experimentally studied the influence of substituent effects and established orbital control on these reactions in terms of FMO theory.
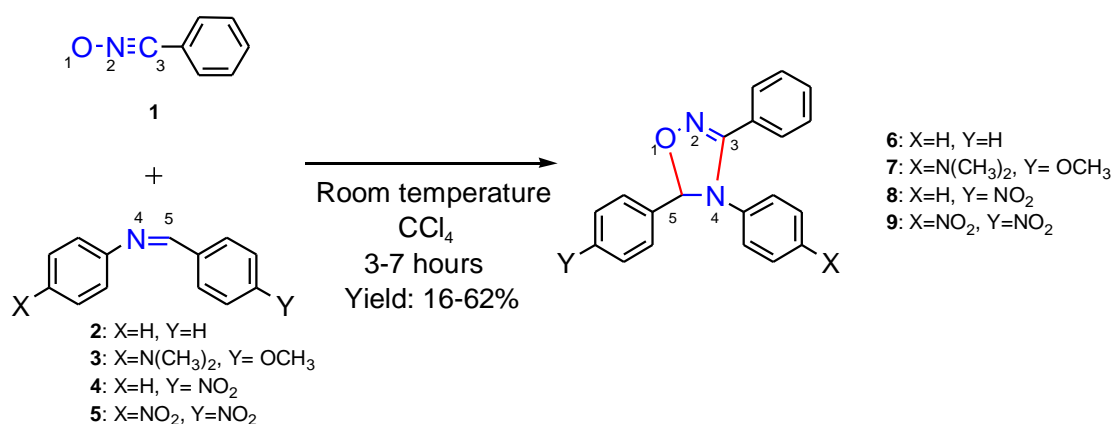
Scheme 1: 32CA reactions of benzonitrile N-oxide BNO **1** to benzylideneanilines **2-5**

With the evolution of computational sciences, software applications for reaction studies have been focused extensively since the last two decades [7], allowing theoretical chemists to establish precise mechanistic implications. In 2016, Domingo proposed the molecular electron density theory [8] (MEDT) to establish the role of electron density changes on molecular reactivity. Since last seven years, the MEDT perspective has been successfully applied to analyse the experimentally observed region [9,10], stereo- [9-12] and chemoselectivity [13,14], reactivity [15-17], substituent effects [18,19], catalysis [20,21], strain promotion [22,23] and several other aspects of 32CA reactions [24,25]. Recently, we have reported the MEDT analysis of the chemo and regioselectivity observed in the 32CA reaction of 4-chlorobenzonitrile N-oxide and β-aminocinnamonitrile for construction of 1,2,4-oxadiazoles [26]. In 2022, Żmigrodzka et al. [27] presented the combined experimental and computational studies on the polar 32CA reaction of N-methyl azomethine ylide and trans-3,3,3-trichloro-1-nitroprop-1-ene. The fruitful interplay of experiment and theory in the 32CA reactions of benzonitrile N-oxide have also been recently reported with the MEDT perspective

[28-30]. Herein, we present a detailed MEDT study for the 32CA reaction of BNO **1** to benzylideneanilines **2-5** (Scheme 1) with the primary aim to interpret the influence of substituents in the aromatic rings of benzylideneanilines. Experimentally, the inclusion of electron releasing dimethylamino and methoxy substituents in the aromatic rings of **3** induce 2.3 fold increase in the reaction rate related to the unsubstituted benzylideneaniline **2**, while the relative rate of **5** bearing two nitro substituents in the aromatic ring is 0.9 relative to **2**.

The present MEDT report is presented in four sections (1) at first, the electron localization function [31-32] (ELF) topological analysis is performed to study the electronic structure at the ground state (GS) of the reagents **1-5** (2) second, the conceptual density functional theory [33-34] (CDFT) indices of the reagents are analysed to predict the electronic flux and polar character (3) then the potential energy surface (PES) along the feasible reaction paths of the studied 32CA reactions are followed to locate the stationary points and the relative enthalpies, entropies and free energies of the products and the transition states (TSs) and the global electron density transfer [35] (GEDT) at the TSs are calculated to assess the polar character of the reactions (4) finally, the electronic structure of the located TSs are studied using the ELF topological analysis and the interatomic interactions are characterised by calculation of the QTAIM [36,37] (Quantum theory of atoms in molecules) parameters and the non-covalent interaction (NCI [38]) analysis.

Computational methods

Optimization of BNO **1**, benzylideneanilines **2-5**, the products **6-13** and the TSs were performed using Berny analytical gradient optimization method [39] at the B3LYP/6-31G(d) level of theory. The minima along the PES were characterised by the absence of imaginary frequency while the TSs by the presence of one imaginary frequency. Solvent effects in CCl_4 were taken into account by full optimization at B3LYP/6-31G(d)/PCM level of theory within the self-consistent reaction field (SCRF) framework [40-42]. The thermodynamic parameters were calculated at 298 K and 1 atm in accordance with the experimental reaction conditions[6]. The intrinsic reaction coordinate (IRC) pathways [43] were studied using the second order Gonzales-Schlegel integration method [44,45]. GEDT [35] was calculated from the Natural bond orbital (NBO) calculations [46,47] at the TSs using the formula GEDT $(f) = \sum_{q \in f} q$, where q denotes the NBO derived charges. The CDFT indices were calculated in accordance with reference [33]. The relative extent of bond formation at the TSs was determined using l index [48] calculated by Eq. 1

$$l = 1 - [\{r^{TS}_{(A-B)} - r^{P}_{(A-B)}\} / r^{P}_{(A-B)}] \qquad \text{Eq. 1}$$

where the distance between the reacting centres A and B in the TS is given by $r^{TS}_{(A-B)}$, and the distance between the reacting centres A and B in the product is denoted by $r^{P}_{(A-B)}$. All calculations were performed using Gaussian 16 suite of programs [49] and the output files were visualised in GaussView [50]. ELF [31,32] (with a high-quality grid with a spacing of 0.06 Bohr) and QTAIM parameters [36,37] were calculated using the Multiwfn software [51]. ELF attractors and localisation domains were visualised using the UCSF Chimera software [52] at an isovalue 0.82 a.u. and the NCI isosurfaces were visualised using the VMD 1.9.3 [53].

Results and discussion

Analysis of the ground state (GS) electronic structures of the reagents

The electron localization function (ELF) proposed by Becke and Edgecombe [31] allows characterizing the electronic regions in a chemical system and consequently designating the core, bonding and non-bonding ones in accordance with the illustration of Silvi and Savin [32]. Within the MEDT perspective, the ELF analysis is applied to characterise the three atom components (TACs) and accordingly correlate their molecular reactivity in 32CA reactions. The presence of a monosynaptic basin integrating 1 e is identified as a *pseudoradical* [24] centre, while that integrating 2 e designates a carbenoid [54] centre. TACs with two and one *pseudoradical* centres are coined as *pseudodiradical* [55] and *pseudo(mono)radical* [56] ones. The absence of carbenoid or *pseudoradical* centre is characterised as a zwitterionic [9] TAC. The relative reactivity of these TACs follow the order *pseudodiradical* > *pseudo(mono)radical* ≈ carbenoid > zwitterionic. Consequently, the least reactive of the series, namely the zwitterionic ones, require appropriate electrophilic-nucleophilic interactions to overcome the high energy barrier unlike the other three types of TACs. Herein, the ELF of reagents BNO **1** and the benzylideneanilines **2-5** are studied. The ELF localization domains of the reagents are shown in Figure 1 along with the most significant valence basin populations. The presence of V(O1), V'(O1), V''(O1) and V'''(O1) monosynaptic basins associated with the non-bonding electron density at O1, integrating at a total population of 5.70 e, the disynaptic basins, V(N2,C3) and V'(N2,C3) associated with the N2-C3 triple bond, integrating at a total population of 6.00 e and a disynaptic basin V(N2,O1) associated with N2-O1 single bond, integrating 1.52 e characterise the electronic structure of the reacting moiety at BNO **1**. Note that the absence of *pseudoradical* or carbenoid centre characterises BNO **1** as a zwitterionic TAC. The ELF of the benzylideneanilines **2-5** show the presence of two disynaptic basins V(N4,C5) and V'(N4,C5) integrating the total population of 2.97 e - 3.00 e, associated with the underpopulated N4-C5

double bond and the monosynaptic basin V(N4) integrating between 2.56 e: -2.64 e is associated with the non-bonding electron density at N4.
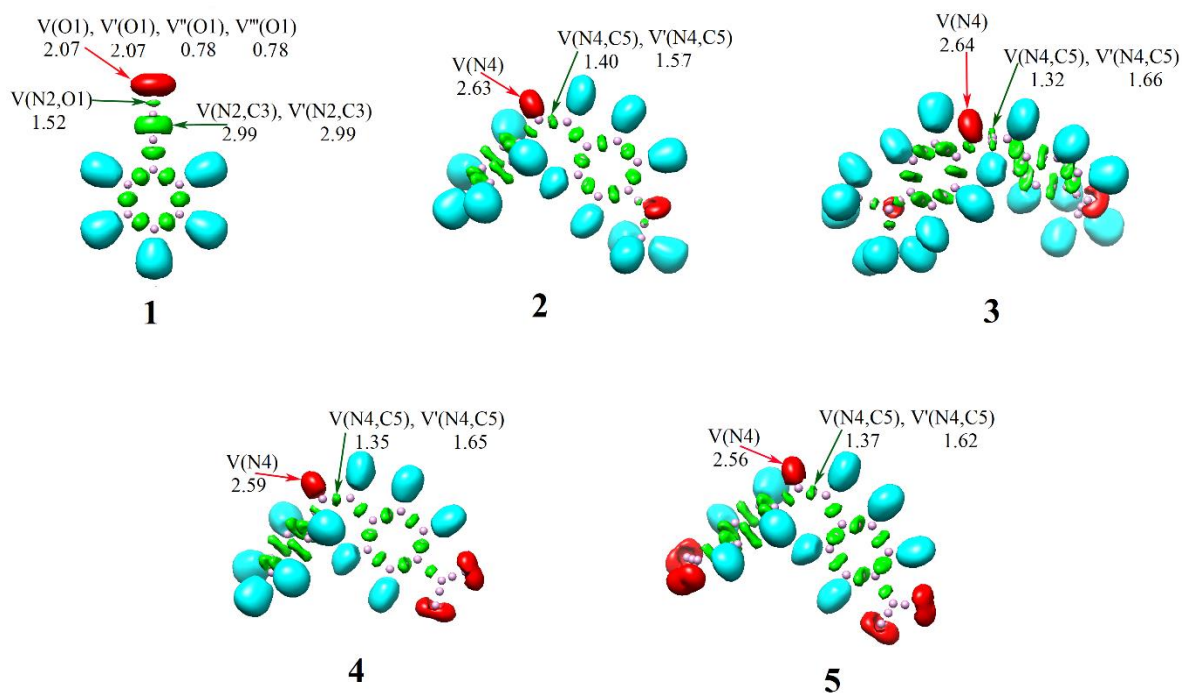

Figure 1. B3LYP/6-31G(d) ELF localization domain (isovalue = 0.82) and the basin attractor positions of reactants **1**-**5**. Protonated basins are shown in blue, monosynaptic basins in red, disynaptic basins in green and core basins in magenta color.

The proposed Lewis-like structures on the basis of ELF study of the reagents **1**-**5** are represented in Figure 2 along with their natural atomic charges. The O1 oxygen atom of BNO **1** is negatively charged by 0.39 e, while N2 nitrogen and C3 carbon atoms are positively charged by 0.17 and 0.22 e. In case of the benzylideneanilines, **2-5**, the N4 nitrogen atoms are negatively charged between 0.40-0.43 e, while the C5 carbon atoms are positively charged between 0.11-0.13 e.
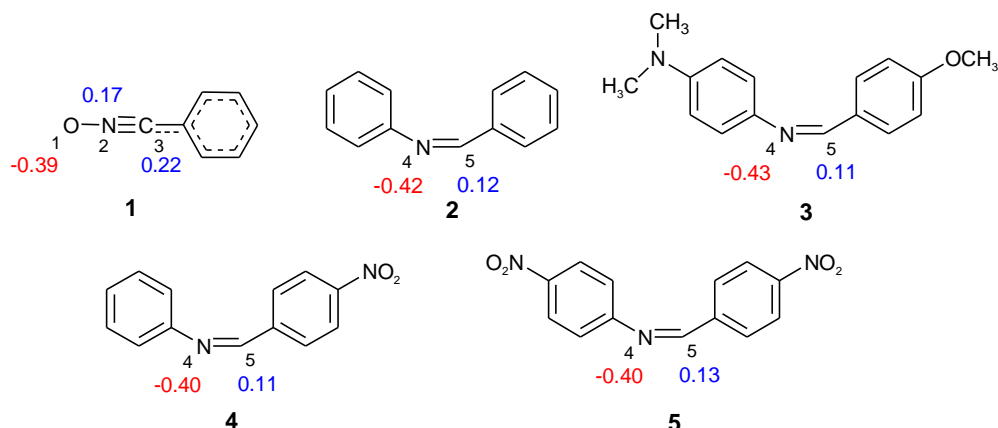

Figure 2. Proposed Lewis-like structures together with the natural atomic charges in average number of electrons, e, of the reactants BNO **1** and benzylideneanilines **2-5**. Negative and positive charges are shown in red and blue colors, respectively.

Analysis of the CDFT indices at the GS of the BNO **1** and benzylidene anilines **2-5**

The CDFT [33,34] analysis has been applied in numerous 32CA reactions [9-26] to assess the electronic behavior at the GS of the reagents and accordingly predict the polar character of the reactions. The electronic chemical potential μ, global electrophilicity ω, chemical hardness η and global nucleophilicity N calculated at the GS of the reagents at the B3LYP/6-31G(d) computational level are given in Table 1.

Table 1. B3LYP/6-31G(d) electronic chemical potential μ, chemical hardness η, electrophilicity ω, and nucleophilicity N, in eV, of the reactants **1**- **5.**

	μ	η	ω	N
1	-3.82	5.03	1.45	2.78
2	-3.37	4.41	1.29	3.54
3	-2.91	3.70	1.15	4.35
4	-4.49	3.27	3.09	2.99
5	-5.02	3.62	3.48	2.29

The electronic chemical potential μ [57] of BNO **1** (μ= -3.82 eV) is less than that of benzylideneanilines **2** (μ= -3.37 eV) and **3** (μ= -2.91 eV) indicating electronic flux from the benzylideneanilines **2** and **3** to BNO **1**, while the small difference in electronic chemical potentials suggests low polar character of the corresponding 32CA reactions. On the other hand, μ of BNO **1** is greater than that of **4** (μ= -4.49 eV) and **5** (μ= -5.02 eV), suggesting electronic flux from BNO **1** to the benzylideneanilines **4** and **5** . The electrophilicity ω [58,59] and nucleophilicity N [55] indices of BNO **1** are 1.45 and 2.78 eV, respectively, allowing its classification as a moderate electrophile (0.80 eV < ω < 1.50 eV) and a moderate nucleophile (2.00 eV < N < 3.00 eV). The electrophilicity ω index of benzylideneanilines **2** and **3** are 1.29 and 1.15 eV, being classified as moderate electrophiles and the nucleophilicity N index are 3.54 and 4.35 eV being classified as the strong nucleophiles (N > 3.00 eV) within the standard electrophilicity [59] and nucleophilicity [60] scales. The electrophilicity ω of benzylideneanilines **4** and **5** are 3.09 and 3.48 respectively being classified as strong electrophiles and the corresponding nucleophilicity indices are 2.99 and 2.29 eV, respectively, classified as moderate nucleophiles. Note that the presence of electron withdrawing nitro substituents in **4** and **5** considerably increases the electrophilicity and decreases the electronic chemical potential, while the presence of electron releasing dimethylamino and methoxy substituents in **3** decreases the electrophilicity and increases the electronic chemical potential relative to the unsubstituted benzylideneaniline **2**, suggesting the influence of substituents on the electronic behavior of the benzylideneanilines.

Exploring the potential energy surface (PES) along the *zw-type* 32CA reaction of BNO **1** with benzylideneanilines **2-5**
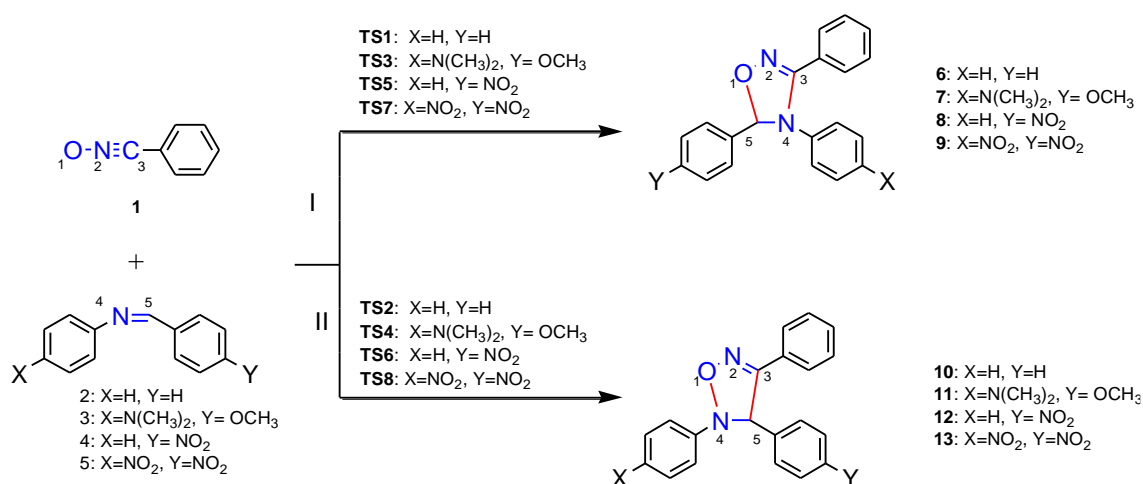
Scheme 2. Studied reaction paths associated with the 32CA reactions of BNO **1** and benzylideneanilines **2-5**

The 32CA reaction of BNO **1** and benzylideneanilines **2-5** can take place along two regioisomeric reaction paths I and II. Path I and Path II are associated respectively with the addition of C3 of BNO **1** to N4 and C5 of the benzylideneanilines (Scheme 2). Search for the stationary points along these two reaction paths allowed location of the reagents **1-5**, products **6-13** and transition states (TSs) **TS1-TS8** along the potential energy surface of each 32CA reaction. Location of one TS revealed one-step mechanism in each case. The relative enthalpies, entropies and free energies of the TSs and the products in CCl_4 at room temperature are given in Table 2. Analysis of the thermodynamic profile allows arriving at some interesting conclusions (i) The 32CA reaction between BNO **1** and the reagents **2-5** along the reaction path I shows negative reaction Gibbs free energies between -13.1 and -15.5 kcal mol^{-1} suggesting exergonic character under kinetic control. On the other hand, the reaction free energies along path II are positive between 13.5 and 17.0 kcalmol^{-1} suggesting endergonic reaction. The reaction free energies of products **6**, **7**, **8** and **9** are lowered than their relative regioisomers **10**, **11**, **12** and **13** by 26.6-32.4 kcalmol^{-1} and the corresponding reaction enthalpies are lowered between 26.8 and 31.5 kcalmol^{-1}, indicating the feasible generation of the cycloadducts through path I in complete agreement with the experiments[6]. (ii) The activation free energy of **TS3** and **TS5** is lowered than that of **TS1** by 2.7 and 2.2 kcal mol^{-1} consistent with the experiments showing higher relative rate constant of **3** and **4** relative to **2**, while that of **TS1** is lowered than that of **TS7** by only 0.4 kcal mol^{-1} consistent with the comparable rate constant 0.9 of **5** relative to **2**. Note that electron releasing

substituents -NMe$_2$ and -OMe make the reaction more feasible relative to the unsubstituted one, while electron withdrawing nitro substitution shows minimal influence on the reaction feasibility (iv) the activation free energies along path I are increased by 14-14.3 kcalmol^{-1} relative to the activation enthalpies due to presence of unfavourable entropies in these bimolecular 32CA reactions.

Table 2. B3LYP/6-31G(d) relative enthalpies (ΔH, in kcal·mol^{-1}), entropies (ΔS, in cal·mol^{-1}K^{-1}) and Gibbs free energies (ΔG, in kcal·mol^{-1}), computed in CCl$_4$, of the stationary points involved in the 32CA reaction of BNO **1** and benzylideneanilines **2-5** along with GEDT in average number of electrons, bond development index ($l_{C3-N4/C3-C5}$ and $l_{O1-C5/O1-N4}$) and differences between the bond development index (Δl) at the **TS1-TS8**.

	ΔH	ΔS	ΔG	GEDT	$l_{C3-N4/C3-C5}$	$l_{O1-C5/O1-N4}$	Δl
TS1	10.4	-47.3	24.5	0.06	0.559	0.245	0.314
6	-29.1	-49	-14.5				
TS2	20.4	-47.7	34.6	0.03	0.723	0.397	0.327
10	-1.1	-50	13.8				
TS3	7.8	-46.8	21.8	0.09	0.566	0.227	0.34
7	-30.0	-48.8	-15.5				
TS4	17.9	-43.7	31	0.03	0.702	0.313	0.39
11	-0.6	-47.8	13.7				
TS5	8.0	-48	22.3	0.02	0.565	0.329	0.237
8	-29.7	-48.1	-15.4				
TS6	27.3	-47.2	41.4	0.07	0.711	0.462	0.249
12	1.8	-50.9	17				
TS7	10.6	-48.2	24.9	0.01	0.562	0.462	0.100
9	-28.4	-51.3	-13.1				
TS8	19.7	-46.8	33.6	0.12	0.746	0.453	0.292
13	-1.6	-50.6	13.5				

The B3LYP/6-31G(d) optimized geometry of the TSs associated with the 32CA reactions are given in Figure 3. The forming C-O bond distances in **TS1**, **TS3**, **TS5** and **TS7** are 2.478, 2.497, 2.378, and 2.354 Å in gas phase and 2.525, 2.549, 2.398 and 2.268 Å in CCl$_4$, while the forming C-N bond distances are 2.016, 2.000, 2.006 and 2.029 Å in gas phase and 2.012, 1.997, 2.005 and 2.026 Å in CCl$_4$, suggesting minimal solvents effects on the bond distances. The forming bond distances are greater than 2.0 Å, implying that the formation of C-N and C-O bond distances have not been started at these early TSs [24]. In each case, the bond development index [48] $l_{C3-N4/C3-C5}$ is greater than that of $l_{O1-C5/O1-N4}$, suggesting earlier C3-N4/C3-C5 bond formation relative to the forming O1-C5/O1-N4 bond. The asymmetric index Δa denotes the difference between the bonding development index $l_{C3-N4/C3-C5}$ and $l_{O1-C5/O1-N4}$ and measures the extent of asynchronicity in the bond formation process [48]. The polar character of these 32CA reactions were evaluated from the global

electron density theory [35] (GEDT) calculations. GEDT values higher than 0.2 e are indicative of the polar character, while those less than 0.05 e imply non-polar character. Herein, the GEDT at **TS1** and **TS3** are 0.06 and 0.09 indicating that the 32CA reaction of BNO **1** with **2** and **3** show low polar character, while that of **TS5** and **TS7** are 0.02 and 0.01 e indicating that the 32CA reaction of BNO **1** with **4** and **5** show non-polar character.
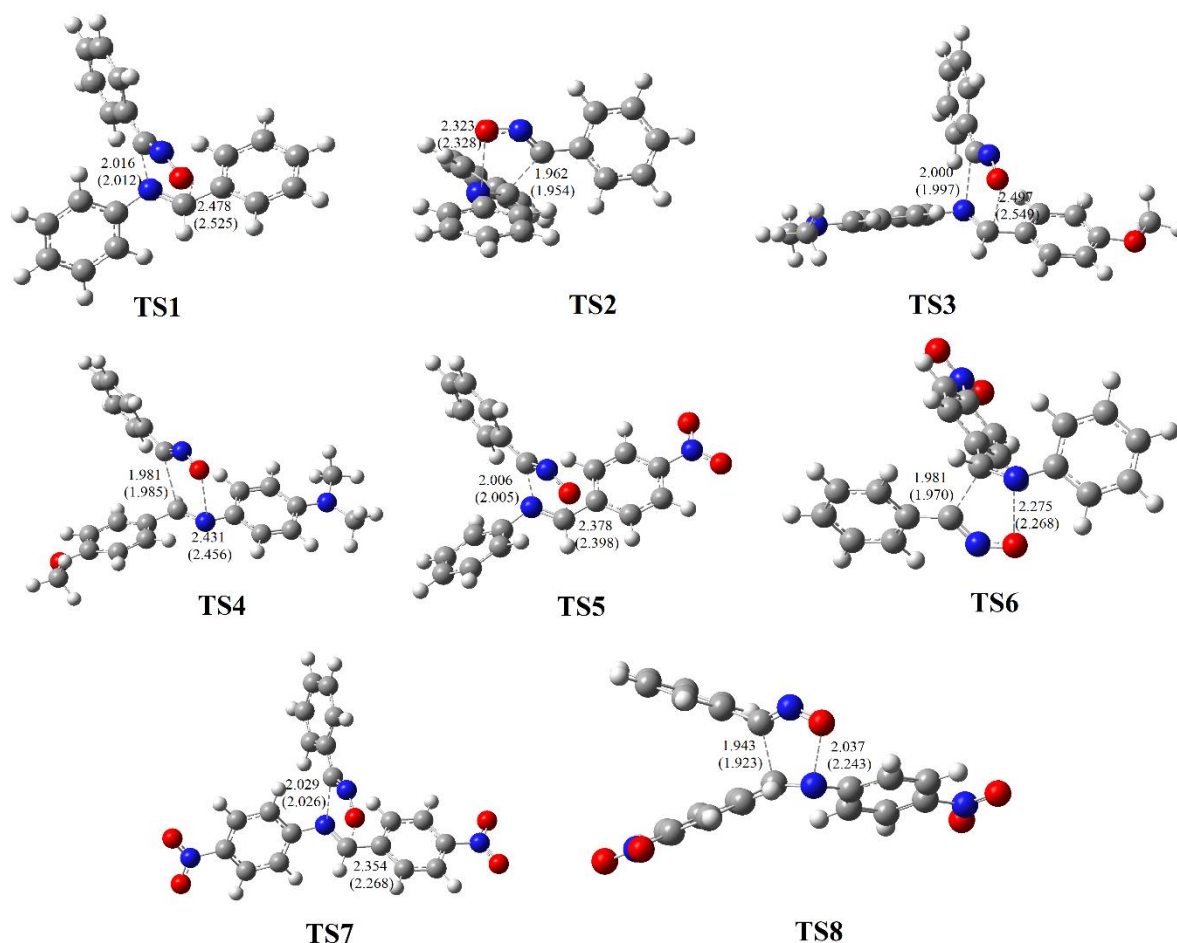

Figure 3. B3LYP/6-31G(d) optimized gas phase geometries of TSs associated with the 32CA reaction of BNO **1** and benzylideneanilines **2-5**. Distances are given in angstroms. Distances in CCl₄ are given in parentheses.

Topological analysis of the ELF and AIM at the TSs

The ELF [31,32] topological analysis at the TSs was performed to study the electronic structure. The most significant ELF valence basin populations and the ELF localization domains are represented in Figure 4, The ELF study at the TSs allowed arriving at some appealing conclusions (1) The ELF of **TS1** shows the presence of one disynaptic V(N2,C3) basin integrating 3.47 e, indicating depopulation of 2.53 e of the N2-C3 bonding region relative to BNO **1**. Similarly, the N2-C3 bonding region is depopulated between 1.86-2.90 e at **TS2-TS8** relative to BNO **1** indicating rupture of the N2-C3 triple bond at the TSs (2) The ELF of **TS1-TS8** also shows the presence of monosynaptic V(N2) basin integrating between

2.10 (**TS8**) and 2.32 e (**TS3**) associated with the accumulation of non bonding electron density at N2 nitrogen deriving electron density from the C3-N2 bonding region. (3) The ELF of **TS1** doesn't show the presence of monosynaptic V(C3) basin, while **TS3**, **TS5** and **TS7** show the presence of monosynaptic V(C3) basins associated with the formation of *pseudoradical* centre at C3. (4) The ELF of **TS2**, **TS4**, **TS6** and **TS8** show the presence of monosynaptic basins V(C3) and V(C5) associated with the *pseudoradical* centres at C3 and C5 (5) The ELF of TSs do not show the disynaptic basins corresponding to the formation of new covalent bonds, consistent with the forming bond distances greater than 2.0 Å (Figure 3).
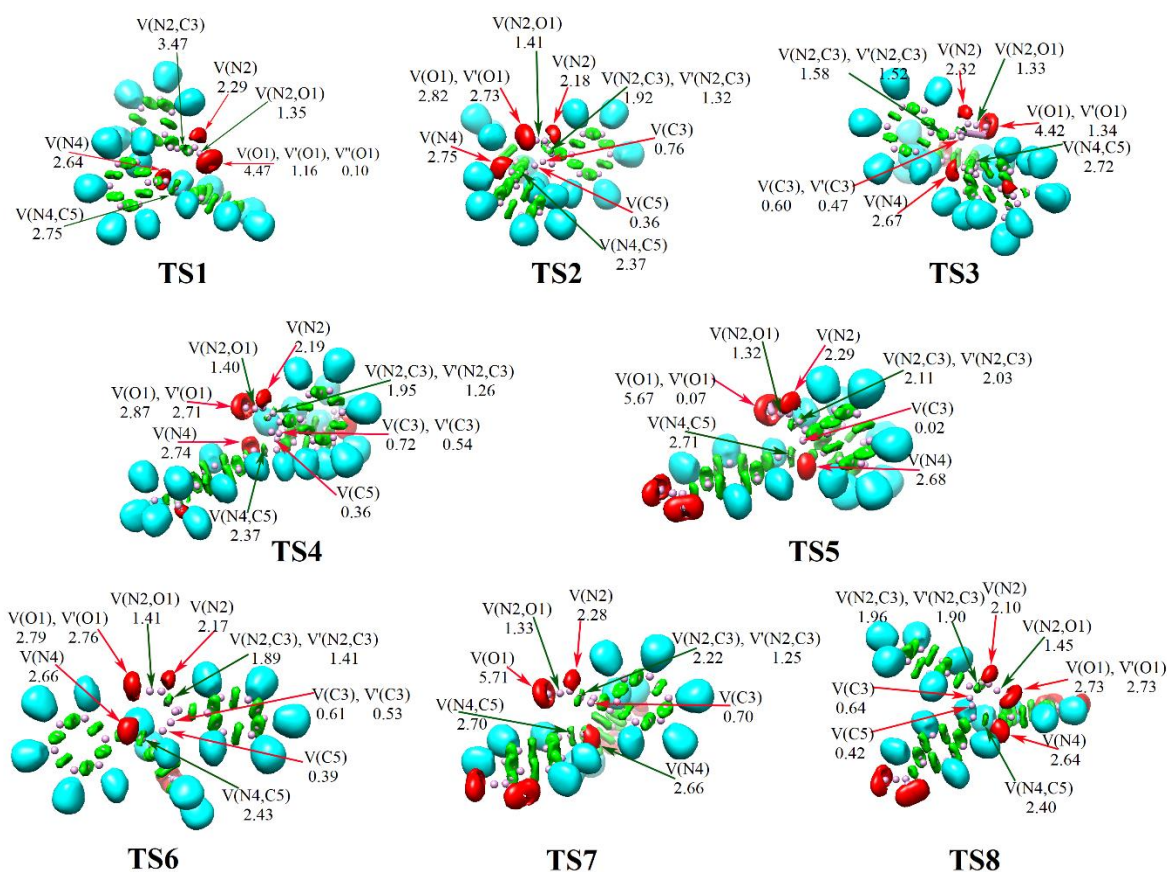
Figure 4. B3LYP/6-31G(d) ELF basin attractor positions and the most significant ELF valence basin populations of **TSs** associated with the 32CA reaction of BNO **1** and benzylideneanilines **2-5**

The AIM [36,37] topological analysis was performed to predict the interatomic interaction at the TSs. total electron density, ρ (e·Å^{-3}), and Laplacian of electron density, $\nabla^2\rho(r_c)$ (e·Å^{-5}) at the TSs and are given in Table 3. The bond critical points **BCP1** and **BCP2** at the TSs are respectively located at the interatomic regions associated with the forming C3-N4/C3-C5 and O1-C5/O1-N4 bonds. The total electron density ρ less than 0.1 e and positive Laplacian of electron density (except minimally negative at **BCP1** of **TS2**) at the TSs indicate non-covalent interactions at the TSs, consistent with the ELF study and the

forming bond distances revealing that the formation of covalent bonds has not been started at the TSs. The NCI isosurfaces at the TSs are shown in Figure 5. The green isosurfaces indicate weak non-covalent interactions at the TSs.

Table 3. B3LYP/6-31G(d) total electron density, ρ (e·Å^{-3}), and Laplacian of electron density, $\nabla^2\rho(r_c)$ (e·Å^{-5}), at **BCP1** and **BCP2** of the TSs associated with the 32CA reaction of BNO **1** and benzylideneanilines **2-5**.

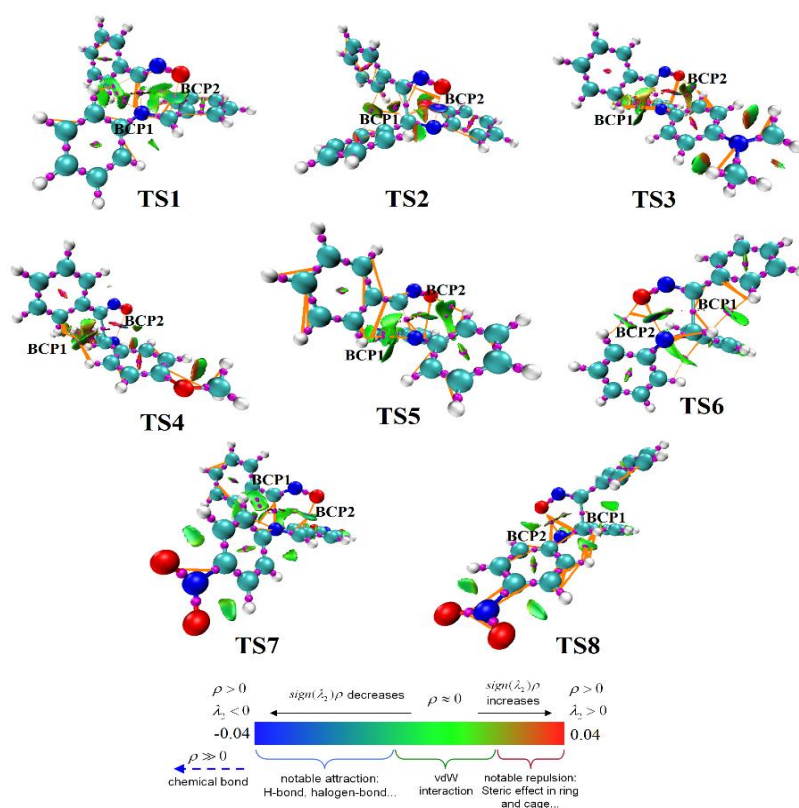| Gas Phase TSs	**BCP1**(C3-N4/C3-C5)		**BCP2**(O1-C5/O1-N4)	
	ρ	$\nabla^2\rho(r_c)$	ρ	$\nabla^2\rho(r_c)$
TS1	0.078	0.101	0.028	0.071
TS2	0.093	-0.003	0.037	0.116
TS3	0.080	0.098	0.027	0.069
TS4	0.090	0.004	0.030	0.090
TS5	0.079	0.097	0.034	0.085
TS6	0.090	0.001	0.041	0.130
TS7	0.076	0.100	0.035	0.088
TS8	0.097	-0.001	0.067	0.206

Figure 5. NCI isosurfaces (isovalue = 0.5), in the range 0.04 < sign(λ_2)ρ < 0.04 a.u., of **TSs** associated with the 32CA reactions of BNO **1** and benzylideneanilines **2-5.**

Conclusion

The 32CA reactions of benzonitrile N-oxide (BNO) **1** with benzylideneanilines **2-5** have been studied at the B3LYP/6-31G(d) level of theory. Topological analysis of the ELF allows to classify the *zw-* type reactivity of BNO **1**, and the CDFT analysis suggests lower electronic chemical potential of BNO **1** relative to the benzylideneanilines **2** (unsubstituted) and **3** (consisting of electron releasing dimethylamino and methoxy substitution at the aromatic rings). On the other hand, the electronic chemical potential of BNO **1** is higher than that of the benzylideneanilines **4** and **5** bearing nitro substituents. BNO **1**, and the benzylideneanilines **2** and **3** are classified as a moderate electrophile, while **4** and **5** are classified as strong electrophiles, indicating the influence of aromatic substitution on the electronic behaviour of the benzylideneanilines. Analysis of the PES along the reaction path suggests exergonic character of the addition along the O1-C5/C3-N4 regioisomeric path and the activation free energies of the TSs follow the order **TS3** > **TS5** > **TS1** > **TS7**, consistent with the experimentally observed relative reaction rates implying facile reaction due to introduction of the electron releasing substituents in the aromatic rings and minimal influence of the electron withdrawing nitro substituents. These 32CA reactions follow one-step mechanism with asynchronicity and the asymmetric index of the forming new bonds are between 0.10 to 0.39. The GEDT at the TSs reveal that the 32CA reactions of **2** and **3** show low polar character, while that of **4** and **5** are non-polar ones. Topological analysis of the ELF suggests that the activation energy is associated with the formation of *pseudoradical* centre at C3 and accumulation of non-bonding electron density at N2 nitrogen by depopulation of the C3-N2 bonding electron density along the reaction path and the formation of new covalent bonds have not been started at the TSs. The NCI analysis characterises weak non-covalent interactions at the TSs revealed from the total electron density and positive Laplacian at the BCPs associated with the forming C-N and C-O bonds.

References

[1] Breugst, M.; Reissig, H.U.; The Huisgen Reaction: Milestones of the 1,3-Dipolar Cycloaddition, *Angew. Chem. Int. Ed.* **2020**, 59, 12293-12307. DOI:10.1002/anie.202003115

[2] Padwa, A.; Pearson, W. H. Synthetic Application of 1,3-Dipolar Cycloaddition Chemistry Toward Heterocycles and Natural Products. **2002**, Wiley: New York.

[3] Feuer, H.; Nitrile Oxides, Nitrones, and Nitronates in Organic Synthesis: Novel Strategies in Synthesis. **2007**, John Wiley & Sons, Inc. DOI:10.1002/9780470191552

[4] Eckell, A.; Huisgen, R.; Sustmann, R.; Wallbillich, G.; Grashey, D.; Spindler, E.; 1.3-Dipolare Cycloadditionen, XXXI. Dipolarophilen-Aktivitäten gegenüber Diphenylnitrilimin und zahlenmäßige Ermittlung der Substituenteneinflüsse. *Chem. Ber*. **1967,** 100, 2192-2213. DOI: 10.1002/Cber.19671000714

[5] Hemming, K.; Recent developments in the synthesis, chemistry and applications of the fully unsaturated 1,2,4-oxadiazoles. *J. Chem. Res. Synop*. **2001**, 6, 209–221. DOI: 10.3184/030823401103169603

[6] Alcaide, B.; Mardomingo, C. L.; Plumet J.; Cativiela C.; Mayoral, J. A.; Orbital control in the 1,3-dipolar cycloaddition of benzonitrile oxide to benzylideneanilines. *Can. J. Chem.* **1987,** 65, 2050-2056. DOI: 10.1139/v87-340

[7] Krylov, A.; Windus, T.L.; Barnes, T.; Rimoldi, E.M-.; Nash, J.A.; Pritchard, B.; Smith, D. G. A.; Altarawy, D.; Saxe, P.; Clementi, C.; Crawford, T.D.; Harrison, R.J.; Jha, S.; Pande, V.S.; Gordon,T.H. Perspective: Computational chemistry software and its advancement as illustrated through three grand challenge cases for molecular science. *J. Chem. Phys*. **2018**, *149*, 180901-1-11. DOI: 10.1063/1.5052551

[8] Domingo, L. R.; Molecular Electron Density Theory: A Modern View of Reactivity in Organic Chemistry. *Molecules* **2016,** 21, 1319. DOI: 10.3390/molecules21101319

[9] Domingo, L. R.; Ríos-Gutiérrez, M.; Pérez, P.; A Molecular Electron Density Theory Study of the Reactivity and Selectivities in [3 + 2] Cycloaddition Reactions of C,N-Dialkyl Nitrones with Ethylene Derivatives. *J. Org. Chem.* **2018**, 83, 2182-2197. DOI: 10.1021/acs.joc.7b03093

[10] Domingo, L.R.; Ríos-Gutiérrez, M.; Adjieufack, A.I.; Ndassa, I.M.; Nouhou, C.N.; Mbadcam, J.K. Molecular Electron Density Theory Study of Fused Regioselectivity in the Intramolecular [3+2] Cycloaddition Reaction of Nitrones. *ChemistrySelect* **2018**, *3*, 5412–5420. DOI: 10.1002/slct.201800224

[11] Acharjee N., Salim H. A. M., Chakraborty M., Rao M. P., Ganesh M.; Unveiling the high regioselectivity and stereoselectivity within the synthesis of

spirooxindolenitropyrrolidine: A molecular electron density theory perspective, *J. Phys. Org. Chem.* **2021**, e4189. DOI: 10.1002/poc.4189

[12] Acharjee, N.; Unravelling the regio- and stereoselective synthesis of bicyclic N,O-nucleoside analogues within the molecular electron density theory perspective, *Struct. Chem.* **2020,** 31, 2147-2160. DOI: 10.1007/s11224-020-01569-x

[13] Domingo, L. R., RiozGutiérrez, M., Acharjee N.; A Molecular Electron Density Theory Study of the Chemoselectivity, Regioselectivity, and Diastereofacial Selectivity in the Synthesis of an Anticancer Spiroisoxazoline derived from α-Santonin, *Molecules* **2019,** 24, 832. DOI: 10.3390/molecules24050832

[14] Domingo, L. R.; Acharjee, N.; Unveiling the Chemo- and Regioselectivity of the [3+2] Cycloaddition Reaction between 4-Chlorobenzonitrile Oxide and β-Aminocinnamonitrile with a MEDT Perspective, *ChemistrySelect* **2021**, 6, 4521-4532. DOI: 10.1002/slct.202100978

[15] Domingo, L. R.; Ríos-Gutiérrez, M.; Silvi, B.; Pérez, P. The mysticism of pericyclic reactions: A contemporary rationalisation of organic reactivity based on electron density analysis. *Eur. J. Org. Chem*. **2018**, 1107-1120. DOI: 10.1002/ejoc.201701350

[16] Domingo, L. R.; Acharjee, N.; Salim, H. A. M.; Understanding the Reactivity of Trimethylsilyldiazoalkanes participating in [3+2] Cycloaddition Reaction towards Diethylfumarate with a Molecular Electron Density Theory Perspective, *Organics* **2020**, 1, 3-18. DOI:10.3390/org1010002

[17] Acharjee, N.; Mondal, A.; Chakraborty, M.; Unveiling the intramolecular [3 + 2] cycloaddition reactions of C,N-disubstituted nitrones from the molecular electron density theory perspective. *New J. Chem.* **2022**, 46, 7721-7733. DOI: 10.1039/D2NJ00888B

[18] Domingo, L. R.; Acharjee, N.; Unveiling the Substituent Effects in the Stereochemistry of [3+2] Cycloaddition Reactions of Aryl- and Alkyldiazomethylphosphonates with Norbornadiene within a MEDT Perspective, *ChemistrySelect* **2021**, 6, 10722-10733. DOI: 10.1002/slct.202102942

[19] Domingo, L. R.; Acharjee, N.; [3+2] Cycloaddition Reaction of C-Phenyl-N‑methyl Nitrone to Acyclic-Olefin-Bearing-Electron-Donating Substituent: A Molecular Electron Density Theory Study, *ChemistrySelect* **2018,** 3, 8373-8380. DOI: 10.1002/slct.201801528

[20] Domingo, L. R.; Rioz-Gutiérrez, M.; Acharjee N.; A Molecular Electron Density Theory Study of the Lewis Acid Catalyzed [3+2] Cycloaddition Reactions of Nitrones with Nucleophilic Ethylenes**,** *Eur. J. Org. Chem*. **2022,** e202101417. DOI: 10.1002/ejoc.202101417

[21] Domingo, L. R.; Rioz-Gutiérrez, M.; Pérez, P.; A Molecular Electron Density Theory Study of the Role of the Copper Metalation of Azomethine Ylides in [3 + 2] Cycloaddition Reactions. *J. Org. Chem*. **2018**, 83,10959-10973. DOI: 10.1021/acs.joc.8b01605

[22] Domingo, L. R.; Acharjee, N.; Unravelling the Strain-Promoted [3+2] Cycloaddition Reactions of Phenyl Azide with Cycloalkynes from the Molecular Electron Density Theory Perspective, *New J. Chem.* **2020,** 44, 13633-13643. DOI: 10.1039/D0NJ02711A

[23] Domingo, L. R.; Acharjee, N.; Unveiling the High Reactivity of Strained Dibenzocyclooctyne in [3+2] Cycloaddition Reactions with Diazoalkanes through the Molecular Electron Density Theory, *J. Phys. Org. Chem.* **2020,** 33, e4100. DOI: 10.1002/poc.4100

[24] Ríos-Gutiérrez, M.; Domingo, L. R.; Unravelling the Mysteries of the [3+2] Cycloaddition Reactions. *Eur. J. Org. Chem*. **2019**, 267-282. DOI: 10.1002/ejoc.201800916

[25] Domingo L. R.; Acharjee, N.; in.: Molecular Electron Density Theory: A New Theoretical Outlook on Organic Chemistry in Frontiers in Computational Chemistry (Ed.: Ul-Haq, Z.; Wilson A. K.) **2020**, 174-227. DOI: 10.2174/9789811457791120050007

[26] Domingo, L. R.; Acharjee, N.; Unveiling the Chemo- and Regioselectivity of the [3+2] Cycloaddition Reaction between 4-Chlorobenzonitrile Oxide and β-Aminocinnamonitrile with a MEDT Perspective, *ChemistrySelect* **2021**, 6, 4521-4532. DOI: 10.1002/slct.202100978

[27] Sadowski, M.; Utnicka, J.; Wójtowicz, A.; Kula, K.; The global and local Reactivity of C,N diarylnitryle imines in [3+2] cycloaddition processes with trans-β-nitrostyrene according to Molecular Electron Density Theory: A computational study. *Curr. Chem. Lett.* **2023**, 12, 421–430. DOI: 10.5267/j.ccl.2022.11.004

[28] Zawadzinska, K.; Kula, K. Application of β-Phosphorylated Nitroethenes in [3+2] Cycloaddition Reactions Involving Benzonitrile N-Oxide in the Light of a DFT Computational Study. *Organics* **2021**, 2, 26–37. DOI: 10.3390/org2010003

[29] Żmigrodzka, M.; Sadowski, M.; Kras, J.; Dresler, E.; Demchuk, O.M.; Kula, K.; Polar [3+2] cycloaddition between N-methyl azomethine ylide and trans-3,3,3-trichloro-1-nitroprop-1-ene. *Sci. Rad*. **2022**, 1, 26-35. DOI: 10.58332/v22i1a02

[30] Zawadzińska, K.; Ríos-Gutiérrez, M.; Kula, K.; Woliński, P.; Mirosław, B.; Krawczyk, T.; Jasiński, R. The Participation of 3,3,3-Trichloro-1-nitroprop-1-ene in the [3 + 2] Cycloaddition Reaction with Selected Nitrile N-Oxides in the Light of the Experimental and MEDT Quantum Chemical Study. *Molecules* **2021**, 26, 6774. DOI: 10.3390/molecules26226774

[31] Becke, A. D.; Edgecombe, K. E.; A simple measure of electron localization in atomic and molecular systems. *J. Chem. Phys*. **1990**, 92, 5397. DOI: 10.1063/1.458517

[32] Silvi, B.; Savin, A.; Classification of chemical bonds based on topological analysis of electron localization functions. *Nature* **1994** 371, 683–686. DOI: 10.1038/371683a0

[33] Domingo, L. R.; Ríos-Gutiérrez, M.; Pérez, P.; Applications of the Conceptual Density Functional Theory Indices to Organic Chemistry Reactivity. *Molecules* **2016,** 21, 748. DOI: 10.3390/molecules21060748

[34] Geerlings, P.; Proft, F. D.; Langenaeker, W.; Conceptual Density Functional Theory. *Chem. Rev*. **2003**, 103, 1793-1874. DOI: 10.1021/cr990029p

[35] Domingo, L. R.; A new C–C bond formation model based on the quantum chemical topology of electron density. *RSC Adv*. **2014**, 4, 32415-32428. DOI: 10.1039/C4RA04280H

[36] Bader, R. F. W.; Atoms in Molecules: A Quantum Theory. **1994**, Oxford University Press, Oxford, New York.

[37] Bader, R. F. W.; Essén, H.; The characterization of atomic interactions. *J. Chem. Phys*. **1984**, 80, 1943. DOI:10.1063/1.446956

[38] García, J. C.; Johnson, E. R.; Keinan, S.; Chaudret, R.; Piquemal, J. P.; Beratan, D. N.; Yang, W.; NCIPLOT: A Program for Plotting Noncovalent Interaction Regions. *J. Chem. Theory Comput*. **2011**, 7, 625-632. DOI: 10.1021/ct100641a

[39] Hehre, W. J.; Radom, L.; Schleyer, PvR.; Pople, J.; In: AB INITIO Molecular Orbital Theory, **1986**, Wiley-Interscience, New York.

[40] Tomasi, J.; Persico, M.; Molecular Interactions in Solution: An Overview of Methods Based on Continuous Distributions of the Solvent. *Chem. Rev*. **1994**, 94, 2027-2094. DOI: 10.1021/cr00031a013

[41] Cancès, E.; Mennucci, B.; Tomasi, J.; A new integral equation formalism for the polarizable continuum model: Theoretical background and applications to isotropic and anisotropic dielectrics. *J. Chem. Phys.* **1997**, 107, 3032-3041. DOI: 10.1063/1.474659

[42] Barone, V.; Cossi, M.; Tomasi, J.; Monte-Carlo model for the hydrogenation of alkenes on metal catalyst. *J. Comput. Chem.* **1998**, 19, 404-417. DOI: 10.1002/(SICI)1096-987X(199803)19:4<404::AID-JCC3>3.0.CO;2-W

[43] Fukui, K.; Formulation of the reaction coordinate. *J. Phys. Chem.* **1970**, 74, 4161-4163. DOI: 10.1021/j100717a029

[44] Gonzalez, C.; Schlegel, H. B.; Reaction path following in mass-weighted internal coordinates. *J. Phys. Chem.* **1990**, 94, 5523-5527. DOI: 10.1021/j100377a021

[45] González, C.; Schlegel, H. B.; Improved algorithms for reaction path following: Higher-order implicit algorithms. *Chem. Phys.* **1991**, 95, 5853-5860. DOI: 10.1063/1.461606

[46] Reed, A. E.; Weinstock, R. B.; Weinhold, F.; Natural population analysis. *J. Chem. Phys.* **1985**, 83, 735-746. DOI: 10.1063/1.449486

[47] Reed, A. E.; Curtiss, L. A.; Weinhold, F.; Intermolecular interactions from a natural bond orbital, donor-acceptor viewpoint. *Chem. Rev.* **1988**, 88, 899-926. DOI: 10.1021/cr00088a005

[48] Jasiński, R.; A stepwise, zwitterionic mechanism for the 1,3-dipolar cycloaddition between (Z)-C-4-methoxyphenyl-N phenylnitrone and gem-chloronitroethene catalysed by 1-butyl-3-methylimidazolium ionic liquid cations. *Tetrahedron Lett.* **2015**, 56, 532-535. DOI: 10.1016/j.tetlet.2014.12.007

[49] Frisch, M.; Trucks, G.; Schlegel, H.; Scuseria, G.; Robb, M.; Cheeseman, J.; Scalmani, G.; Barone, V.; Petersson, G.; Nakatsuji, H.; Gaussian 16. Revision A, **2016**, 3.

[50] Dennington, Roy; Keith, Todd A.; Millam, John M.; GaussView, Version 6, Semichem Inc., Shawnee Mission, KS, **2016**.

[51] Lu, T.; Chen, F.; Multiwfn: A multifunctional wavefunction analyzer. *J. Comput. Chem.* **2012**, 33:580-592. DOI: https://doi.org/10.1002/jcc.22885

[52] Pettersen, E. F.; Goddard, T. D.; Huang, C. C.; Couch, G. S.; Greenblatt, D. M.; Meng, E. C.; Ferrin, T. E.; UCSF Chimera—A visualization system for exploratory research and analysis. *J. Comput. Chem.* **2004**, 25,1605-1612. DOI: 10.1002/jcc.20084

[53] Humphrey, W.; Dalke, A.; Schulten, K.; VMD: Visual molecular dynamics. *J. Mol. Graph.* **1996**, 14, 33-38. DOI: 10.1016/0263-7855(96)00018-5

[54] Ríos-Gutiérrez, M.; Domingo, L. R.; The carbenoid-type reactivity of simplest nitrile imine from a molecular electron density theory perspective. *Tetrahedron* **2019**, 75, 1961-1967. DOI: 10.1016/j.tet.2019.02.014

[55] Domingo, L. R.; Chamorro, E.; Perez, P.; Understanding the High Reactivity of the Azomethine Ylides in [3+2] Cycloaddition Reactions. *Lett. Org. Chem.* **2010**, 7, 432-439. DOI: 10.2174/157017810791824900

[56] Domingo, L. R.; Ríos-Gutiérrez, M.; A Molecular Electron Density Theory Study of the Reactivity of Azomethine Imine in [3+2] Cycloaddition Reactions. *Molecules* **2017**, 22, 750. DOI: 10.3390/molecules22050750

[57] Parr, R. G.; Yang, W.; Density-functional theory of atoms and molecules. **1989**, Oxford University Press, New York.

[58] Parr, R. G.; Szentpály, L. V.; Liu, S.; Electrophilicity Index*. J. Am. Chem. Soc.* **1999**, 121, 1922-1924. DOI: 10.1021/ja983494x

[59] Domingo, L. R.; Aurell, M. J.; Pérez, P.; Contreras, R.; Quantitative characterization of the global electrophilicity power of common diene/dienophile pairs in Diels–Alder reactions. *Tetrahedron* **2002**, 58, 4417-4423. DOI: 10.1016/S0040-4020(02)00410-6

[60] Domingo, L. R.; Pérez, P.; The nucleophilicity N index in organic chemistry. *Org. Biomol. Chem.* **2011**, 9, 7168-7175. DOI:10.1039/C1OB05856H